

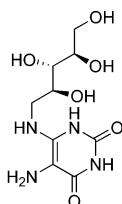
Synthesis and Enzyme Inhibitory Activity of the *S*-Nucleoside Analogue of the Ribitylaminopyrimidine Substrate of Lumazine Synthase and Product of Riboflavin Synthase

Arindam Talukdar,[†] Boris Illarionov,[‡] Adelbert Bacher,[‡] Markus Fischer,[§] and Mark Cushman^{*,†}

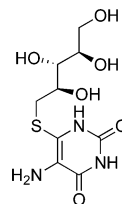
Department of Medicinal Chemistry and Molecular Pharmacology, School of Pharmacy and Pharmaceutical Sciences, and the Purdue Cancer Center, Purdue University, West Lafayette, Indiana 47907, Lehrstuhl für Organische Chemie und Biochemie, Technische Universität München, Lichtenbergstr 4, D-85747 Garching, Germany, and Institut für Lebensmittelchemie, Abteilung Lebensmittelchemie, Universität Hamburg, D-20146 Hamburg, Germany

cushman@pharmacy.purdue.edu

Received May 9, 2007



Lumazine synthase substrate and riboflavin synthase product



Inhibitor of lumazine synthase and riboflavin synthase

Lumazine synthase and riboflavin synthase catalyze the last two steps in the biosynthesis of riboflavin. To obtain structural and mechanistic probes of these two enzymes, as well as inhibitors of potential value as antibiotics, a sulfur analogue of the pyrimidine substrate of the lumazine synthase-catalyzed reaction and product of the riboflavin synthase-catalyzed reaction was designed. Facile syntheses of the *S*-nucleoside 5-amino-6-(*D*-ribitylthio)pyrimidine-2,4(1*H*,3*H*)-dione hydrochloride (**15**) and its nitro precursor 5-nitro-6-(*D*-ribitylthio)pyrimidine-2,4(1*H*,3*H*)-dione (**14**) are described. These compounds were tested against lumazine synthase and riboflavin synthase obtained from a variety of microorganisms. Compounds **14** and **15** were found to be inhibitors of both riboflavin synthase and lumazine synthase. Compound **14** is an inhibitor of *Bacillus subtilis* lumazine synthase (K_i 26 μM), *Schizosaccharomyces pombe* lumazine synthase (K_i 2.0 μM), *Mycobacterium tuberculosis* lumazine synthase (K_i 11 μM), *Escherichia coli* riboflavin synthase (K_i 2.7 μM), and *Mycobacterium tuberculosis* riboflavin synthase (K_i 0.56 μM), while compound **15** is an inhibitor of *B. subtilis* lumazine synthase (K_i 2.6 μM), *S. pombe* lumazine synthase (K_i 0.16 μM), *M. tuberculosis* lumazine synthase (K_i 31 μM), *E. coli* riboflavin synthase (K_i 47 μM), and *M. tuberculosis* riboflavin synthase (K_i 2.5 μM).

Introduction

Riboflavin, vitamin B₂, is involved in many biochemical reactions that are essential for the maintenance of life. Lumazine synthase and riboflavin synthase catalyze the last two steps in the biosynthesis of riboflavin (**4**) (Scheme 1). Higher organisms, including humans, acquire riboflavin through dietary sources, but a variety of pathogenic Gram-negative Enterobacteria and

Candida- and *Saccharomyces*-type yeasts are dependent on endogenous biosynthesis because they do not have efficient riboflavin uptake systems.^{1–4} The inhibition of enzymes involved in riboflavin (**4**) biosynthesis therefore provides a rational strategy for antibiotic drug design.

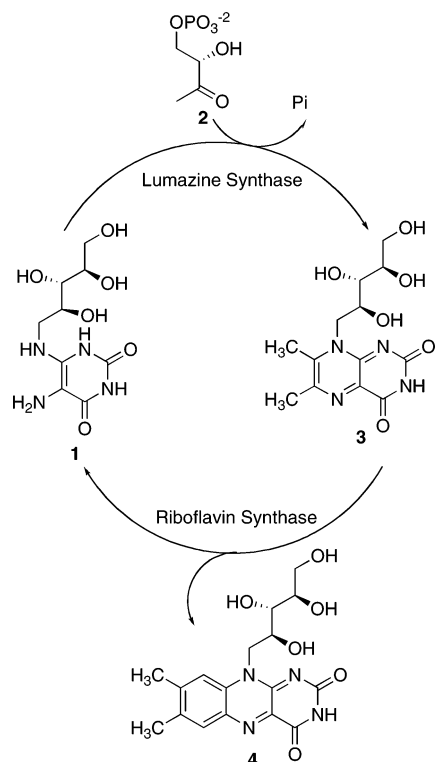
- (1) Wang, A. *I Chuan Hsueh Pao* **1992**, *19*, 362–368.
- (2) Oltmanns, O.; Lingens, F. Z. *Naturforschung* **1967**, *22 b*, 751–754.
- (3) Logvinenko, E. M.; Shavlovsky, G. M. *Mikrobiologiya* **1967**, *41*, 978–979.
- (4) Neuberger, G.; Bacher, A. *Biochem. Biophys. Res. Commun.* **1985**, *127*, 175–181.

[†] Purdue University.

[‡] Technische Universität München.

[§] Universität Hamburg.

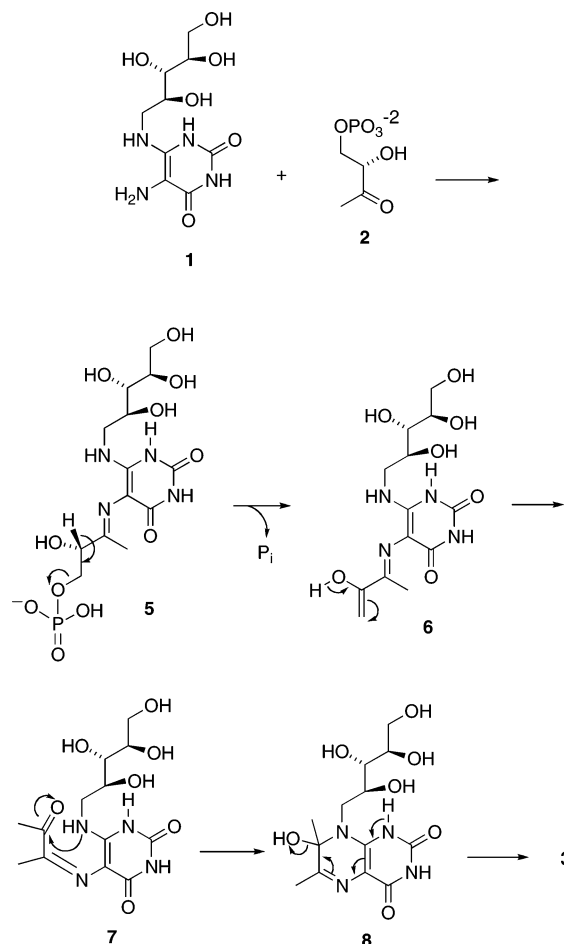
SCHEME 1



The initial steps in the biosynthesis of riboflavin lead from GTP to the pyrimidinedione **1**. Lumazine synthase catalyzes the condensation of 3,4-dihydroxy-2-butanone 4-phosphate (**2**) with 5-amino-6-ribitylamino-2,4(1*H*,3*H*)pyrimidinedione (**1**) yielding 6,7-dimethyl-8-D-ribityllumazine (**3**). The four-carbon phosphate moiety **2** originates from the pentose phosphate pool by the loss of C-4. The riboflavin synthase-catalyzed dismutation of two molecules of 6,7-dimethyl-8-D-ribityllumazine (**3**) results in the formation of one molecule of riboflavin (**4**) and one molecule of the substituted pyrimidinedione **1**, which can be recycled by lumazine synthase. The pyrimidinedione derivative **1** is therefore both a substrate of lumazine synthase and a product of riboflavin synthase.^{5–8} Analogues of **1** could therefore conceivably bind to and inhibit both lumazine synthase and riboflavin synthase.

Although lumazine synthase has been studied for quite some time, the details of its mechanism are not completely known. The initial step of the lumazine synthase-catalyzed reaction requires the presence of the pyrimidinedione **1** substrate in the active site. A hypothetical reaction mechanism is shown in Scheme 2.⁹ It is proposed that the first reaction step is the formation of a Schiff base by reaction of the carbonyl group of **2** with the 5-amino group of **1** yielding the intermediate **5**, which could then eliminate phosphate to form the enol **6**. This intermediate could subsequently tautomerize to **7** and then

SCHEME 2



cyclize to yield the lumazine **3**. Variations of this mechanism are possible depending on the Schiff base geometry and possible isomerization, conformational changes, and the timing of phosphate elimination.

X-ray crystallography of a complex of the phosphonate analogue **9** with lumazine synthase has established that the phosphate of the hypothetical Schiff base binds far away from the ribityl side chain as depicted roughly in chemical structure **5**.¹⁰ The sequence of the phosphate elimination relative to the conformational change of the side chain to form **7** is still not certain. For example, it has recently been proposed that the whole phosphate side chain rotates toward a cyclic conformation with assistance from the enzyme before phosphate elimination and dehydration occur to form the cis Schiff base **7** directly.¹¹ The possible initial formation of a thermodynamically less stable cis Schiff base, or, the isomerization of the trans Schiff base **10** to the cis Schiff base **7**, have not been established. By a semiempirical approach, the energy barrier for the **10** to **7** isomerization was calculated to be 19.6–21 kcal/mol.¹² More recently, in the temperature-dependent pre-steady-state kinetic experiments of lumazine synthase from *Aquifex aeolicus*, it was

(5) Plaut, G. W. E.; Smith, C. M.; Alworth, W. L. *Ann. Rev. Biochem.* **1974**, *43*, 899–922.

(6) Beach, R. L.; Plaut, G. W. E. *J. Am. Chem. Soc.* **1970**, *92*, 2913–2916.

(7) Bacher, A.; Eberhardt, S.; Richter, G. In *Escherichia coli and Salmonella: Cellular and Molecular Biology*, 2nd ed.; Neidhardt, F. C., Ed.; ASM Press: Washington, D.C., 1996; pp 657–664.

(8) Bacher, A.; Fischer, M.; Kis, K.; Kugelbrey, K.; Mörtl, S.; Scheuring, J.; Weinkauff, S.; Eberhardt, S.; Schmidt-Bäse, K.; Huber, R.; Ritsert, K.; Cushman, M.; Ladenstein, R. *Biochem. Soc. Trans.* **1996**, *24*, 89–94.

(9) Volk, R.; Bacher, A. *J. Am. Chem. Soc.* **1988**, *110*, 3651–3653.

(10) Meining, W.; Mörtl, S.; Fischer, M.; Cushman, M.; Bacher, A.; Ladenstein, R. *J. Mol. Biol.* **2000**, *299*, 181–197.

(11) Zhang, X.; Meining, W.; Cushman, M.; Haase, I.; Fischer, M.; Bacher, A.; Ladenstein, R. *J. Mol. Biol.* **2003**, *328*, 167–182.

(12) Zheng, Y. J.; Viitanen, P. V.; Jordan, D. B. *Bioorg. Chem.* **2000**, *28*, 89–97.

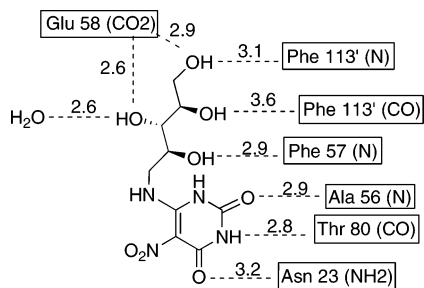
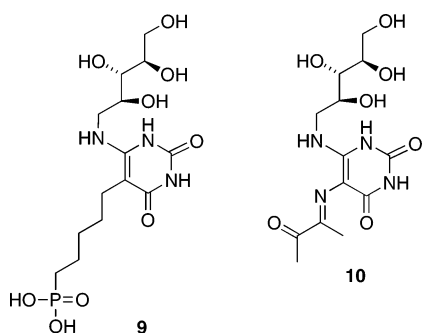


FIGURE 1. Hydrogen bonds and distances of the substrate analogue **11** bound in the active site of *B. subtilis* lumazine synthase. The distances are measured in angstroms.

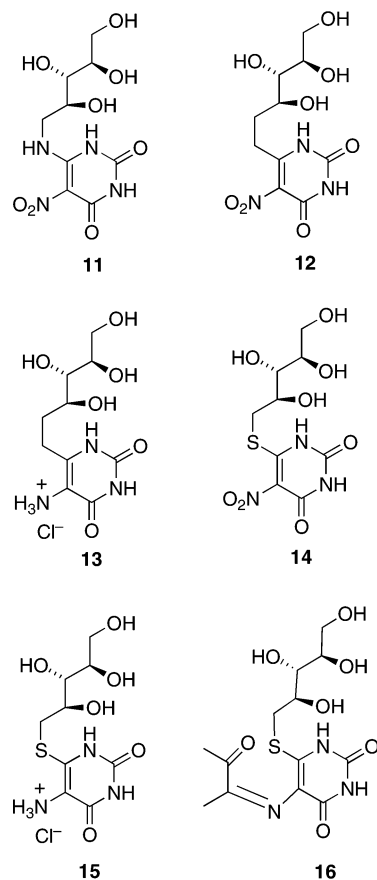
proposed that one of the subsequent steps occurring after phosphate elimination and tautomerization is the rate-determining step.^{13,14}



In order to gain insight into the structural change of the Schiff base side chain occurring after formation of intermediate **5**, substrate analogues are necessary that would allow Schiff base formation but would not allow the cyclization to proceed. The crystal structure of **11** bound to *B. subtilis* lumazine synthase has revealed that the ribitylamino nitrogen has no obvious direct role in binding the ligand to the enzyme (Figure 1), suggesting that the replacement of the nitrogen with another atom might not affect binding to the enzyme.¹⁵ Replacement of the nitrogen atom of the ribitylamino side chain with a heavy atom would not be expected to produce gross changes in the orientation of ribityl chain of **11**, and the resulting compounds could possibly bind to both lumazine synthase and riboflavin synthase. They obviously could not complete the catalytic cycle after reaction with the substrate **2** in the presence of lumazine synthase.

Replacement of the ribitylamino nitrogen of the substrate **1** with carbon was previously reported.¹⁶ The synthesis involved reduction of the nitro compound **12** to afford the C-nucleoside **13**. The nitro analogue **12** displayed inhibitory activity against *B. subtilis* lumazine synthase (K_i 264 μM) and *E. coli* riboflavin synthase (K_i 37 μM). However, surprisingly, the C-nucleoside analogue **13** of the substrate **1** was completely inactive against *B. subtilis* lumazine synthase.¹⁶ Separate binding experiments in the absence of substrate revealed that **13** has essentially no affinity for either lumazine synthase or riboflavin synthase.¹⁶

This observation led to the hypothesis that the nonbonded electrons on the ribitylamino nitrogen atom of the substrate somehow contribute to its binding to lumazine synthase, although as mentioned above, no direct contacts between this nitrogen and the protein are evident in the crystal structure of **11** bound to lumazine synthase.¹⁵ To investigate this in more detail, we decided to prepare the sulfur analogue **15**. If successful, the sulfur analogue **15** might be an effective lumazine synthase inhibitor and it might also be converted to the intermediate analogue **16** in the presence of the substrate **2** and the enzyme. The intermediate analogue **16** might eventually prove to be valuable as a mechanism probe through study of the structure of its complex with the enzyme by kinetics, crystallography, and NMR spectroscopy.



Results and Discussion

For the synthesis of S-nucleoside **14**, the protected ribitol derivative **17** (Scheme 3)¹⁷ was converted to its tosyl derivative **18** by treatment with tosyl chloride in pyridine in the presence of triethylamine and 4-dimethylaminopyridine. The tosyl derivative **18** on exposure to potassium thioacetate in acetonitrile afforded the thioacetate **19**.¹⁸ Reaction of **19** with sodium methoxide in methanol led to a mixture of two products. The NMR spectra of both **20** and **21** did not allow a firm structural assignment. The structures of the expected ribityl sulfide derivative **20** and the disulfide **21** were distinguished by mass spectroscopy. The free sulfide **20** (major) is slightly less polar

(13) Haase, I.; Fischer, M.; Bacher, A.; Schramek, N. *J. Biol. Chem.* **2003**, *278*, 37909–37915.

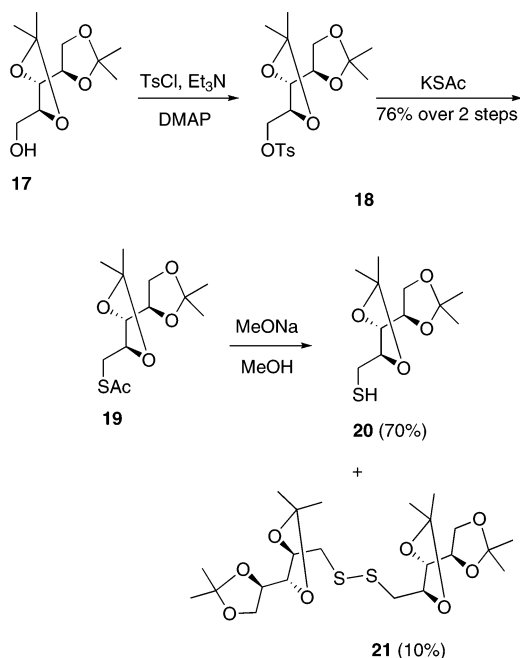
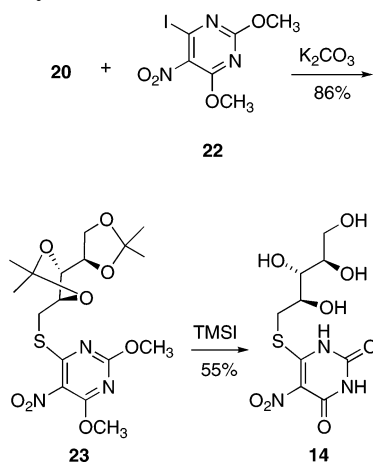
(14) Schramek, N.; Haase, I.; Fischer, M.; Bacher, A. *J. Am. Chem. Soc.* **2003**, *125*, 4460–4466.

(15) Ritsert, K.; Huber, R.; Turk, D.; Ladenstein, R.; Schmidt-Bäse, K.; Bacher, A. *J. Mol. Biol.* **1995**, *253*, 151–167.

(16) Chen, J.; Sambaiah, T.; Illarionov, B.; Fischer, M.; Bacher, A.; Cushman, M. *J. Org. Chem.* **2004**, *69*, 6996–7003.

(17) Amoo, V. E.; Debernardo, S.; Weigele, M. *Tetrahedron Lett.* **1988**, *29*, 2401–2404.

(18) Rahman, A. U.; Daniel, J. R.; Whistler, R. L. *J. Chem. Soc. Pakistan* **1986**, *8*, 397–407.

SCHEME 3. Synthesis of Protected Ribityl Sulfide **20**SCHEME 4. Synthesis of Nitro-*S*-nucleoside Analogue **14**

than the disulfide compound **21** (minor). The sulfide **20** is quite unstable. It is converted to disulfide compound **21** on standing.

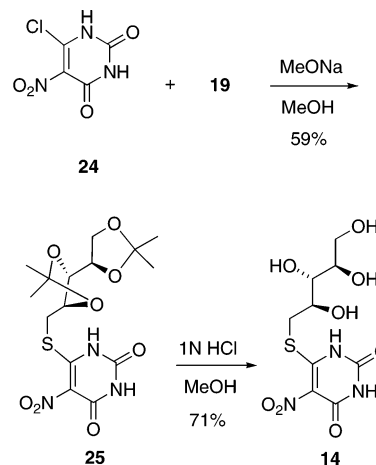
The nucleophilic aromatic substitution reaction between the sulfide **20** and the iodopyrimidine derivative **22**^{19,20} was performed with potassium carbonate as the base (Scheme 4). The reaction occurred efficiently to give sulfide **23** as a white solid in almost quantitative yield. The reaction was improved by addition of 3 equiv of potassium carbonate and use of DMF (instead of THF) as the solvent. The critical simultaneous removal of the isopropylidene and methyl groups from intermediate **23** was accomplished by the treatment of compound **23** with 6 equiv of TMSI.²¹

The TLC of the simultaneous deprotection reaction mixture showed numerous minor spots apart from the major nitro derivative **14**. The purification of the nitro derivative **14** was

(19) Nutiu, R.; Boulton, A. J. *J. Chem. Soc., Perkin Trans. 1* **1976**, 1327–1331.

(20) Sakamoto, T.; Uchiyama, D.; Kondo, Y.; Yamanaka, H. *Chem. Pharm. Bull.* **1993**, *41*, 478–480.

(21) Silverman, R. B.; Radak, R. E.; Hacker, N. P. *J. Org. Chem.* **1979**, *44*, 4970–4971.

SCHEME 5. Facile Synthesis of Nitro-*S*-Nucleoside Analogue **14**

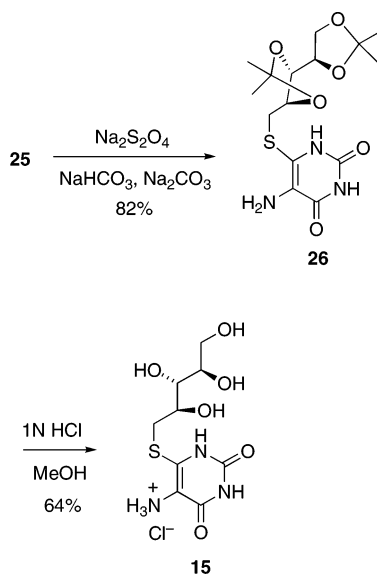
extremely tedious. Compound **14** was column chromatographed several times, finally resulting in a pure, solid compound. Scheme 4 proved to be difficult to execute and the yields were hard to reproduce. These problems prompted the search for an alternative route. Eventually, a more efficient synthesis of the *S*-nucleoside was devised as described in Scheme 5. The thioacetate **19** was treated with an excess of sodium methoxide in MeOH at room temperature for 3 h, which led to the sodium salt of thiol **20**. The excess sodium methoxide facilitates the removal of the acetate group and subsequently converts the free thiol compound into its sodium salt. 6-Chloro-5-nitro-2-methoxyuracil (**24**)²² was introduced, and the reaction mixture was heated at reflux for 12 h to give isopropylidene-protected *S*-nucleoside **25** in good yield. This solved two major problems associated with *S*-nucleoside synthesis. First, it avoids handling the unstable free thiol compound **20**, and second, it also avoids the problem of having to cleave the methoxy groups present in intermediate **23** (Scheme 4).

In order to study the detailed mechanisms of lumazine synthase and riboflavin synthase catalysis, metabolically stable analogues have been sought that can structurally mimic the substrates, hypothetical intermediates, and products involved in 6,7-dimethyl-8-ribityllumazine (**3**) and riboflavin (**4**) biosynthesis. Therefore, the next goal was to reduce the nitro group in **25** to an amino functionality to obtain the desired lumazine synthase substrate analogue and riboflavin synthase product analogue **15**. The resulting compound **15** could possibly bind to lumazine synthase and riboflavin synthase and that would facilitate a study the detailed mechanisms of lumazine synthase and riboflavin synthase catalysis. After trying various conditions, the reduction reaction was successfully carried out using sodium hydrosulfite in the presence of sodium bicarbonate and sodium carbonate in 1,4-dioxane at room temperature to provide amine **26**. The isopropylidene group in the amino compound **26** was readily deprotected using 1 N HCl in MeOH to afford the hydrochloride salt **15** of the desired *S*-nucleoside (Scheme 6).

The *S*-nucleoside analogue **15** of the substrate and product **1**, and its nitro precursor **14**, were evaluated as inhibitors of lumazine synthase of *S. pombe*, *B. subtilis*, and *M. tuberculosis* and of riboflavin synthase of *E. coli* and *M. tuberculosis*. Representative Lineweaver–Burk plots for inhibitor **15** are displayed in Figure 2, and the results calculated for all of the

(22) Cresswell, R. M.; Wood, H. S. C. *J. Chem. Soc.* **1960**, 4768–4775.

SCHEME 6. Synthesis of Amino S-Nucleoside Analogue 15



inhibitors are listed in Table 1. Several additional inhibitors that were previously designed and synthesized to target the ribitylaminopyrimidine binding site of lumazine synthase are also listed in Table 1 for comparison. The S-nucleoside **15** was found to be a potent inhibitor of lumazine synthase of *S. pombe* (K_i 0.16 μM), *B. subtilis* (K_i 2.6 μM), and *M. tuberculosis* (K_i 31 μM) and of riboflavin synthase of *M. tuberculosis* (K_i 2.5 μM), and *E. coli* (K_i 47 μM), whereas the C-nucleoside analogue **13** of the substrate **1** was shown previously to be completely inactive against *B. subtilis* lumazine synthase.¹⁶ The nitro precursor to **15**, compound **14**, was found to be a less potent inhibitor of *B. subtilis* lumazine synthase (K_i 26 μM) and *S. pombe* lumazine synthase (K_i 2.0 μM) than **15**, almost equally potent as an inhibitor of *M. tuberculosis* lumazine synthase (K_i 11 μM) and more potent as an inhibitor of *M. tuberculosis* riboflavin synthase (K_i 0.56 μM) and *E. coli* riboflavin synthase (K_i 2.7 μM) than **15**.

The relative efficacies of the N-nucleoside, C-nucleoside, and S-nucleoside inhibitors can be directly accessed by comparison of the nitro compounds **11**, **12**, and **14** vs *B. subtilis* lumazine synthase (Table 1). Surprisingly, the S-ribityl compound **14** (K_i 26 μM) is almost equally potent as the respective N-ribityl inhibitor **11** (K_i 16 μM) having the natural side chain, and both compounds **14** and **15** (K_i for **15**, 2.6 μM) are much more potent than the respective C-ribityl analogues **12** and **13** (K_i , 309 and >1000 μM). The S-nucleoside **14** is a slightly more potent inhibitor than the N-nucleoside **11** vs *E. coli* riboflavin synthase (K_i 2.7 vs 8.0 μM).

A 2.4 Å resolution X-ray structure is available of the substrate analogue **11** complexed with *B. subtilis* lumazine synthase.¹⁵ The structure allows the construction of a hypothetical model of the binding of **14** to lumazine synthase (Figure 3), which was produced by docking structure **14** into the active site. The energy of the complex was minimized using the MMFF94s force field while allowing the ligand and the protein structure contained within a 6 Å diameter sphere surrounding the ligand to remain flexible with the remainder of the protein structure frozen. The calculated structure of **14** with lumazine synthase suggests that the inhibitor **14** binds in an almost identical fashion to **11** in the active site. The calculated hydrogen bonds and distances between atoms of the substrate analogue **14** and *B. subtilis* lumazine synthase are displayed in Figure 4.

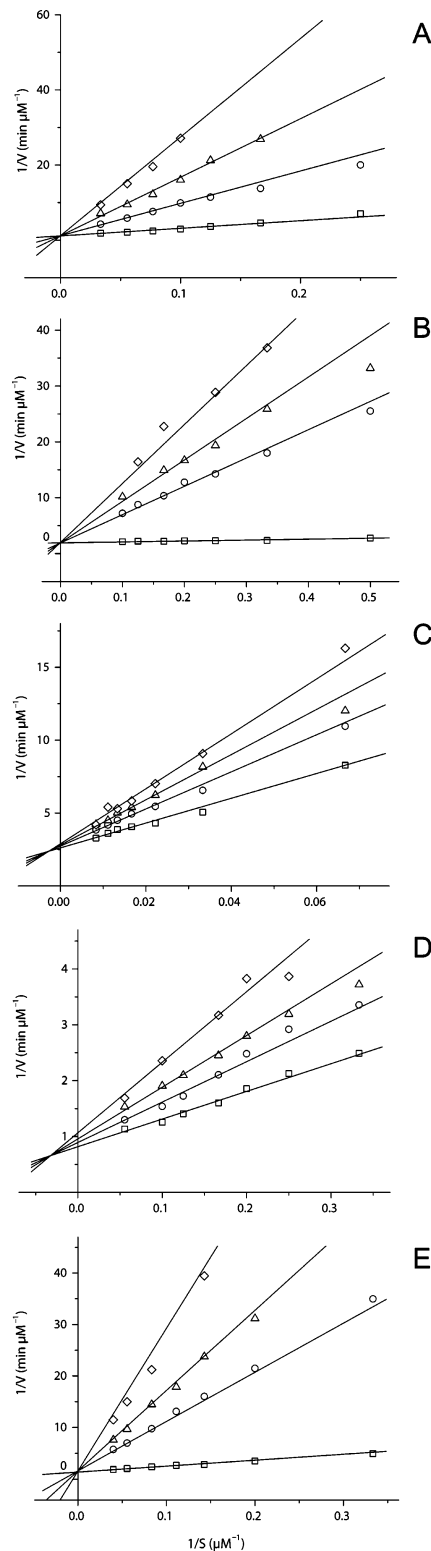
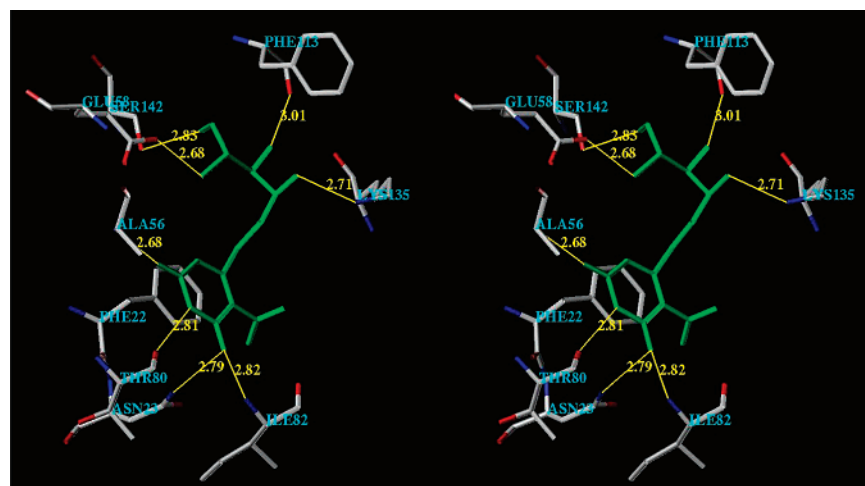


FIGURE 2. Lineweaver-Burk plots for the inhibition of the following enzymes by inhibitor **15**. Lumazine synthases: A, *B. subtilis* (inhibitor concentrations 0, 10, 20, and 40 μM ; mechanism: competitive); B, *S. pombe* (inhibitor concentrations 0, 7, 20, and 60 μM ; mechanism: competitive); C, *M. tuberculosis* (inhibitor concentrations 0, 20, 40, and 80 μM , mechanism: partial). Riboflavin synthases: D, *E. coli* (inhibitor concentrations 0, 20, 40, and 80 μM ; mechanism: partial); E, *M. tuberculosis* (inhibitor concentrations 0, 30, 50, and 90 μM ; mechanism: competitive). The kinetic data were fitted with a nonlinear regression method using the program Dynafit from P. Kuzmic (1996).

TABLE 1. Inhibition Potencies of Synthetic Compounds vs *B. subtilis* Lumazine Synthase,^a *S. pombe* Lumazine Synthase,^b *M. tuberculosis* Lumazine Synthase,^c *E. coli* Riboflavin Synthase,^d and *M. tuberculosis* Riboflavin Synthase^e

compd	enzyme	K_s^f μM	k_{cat}^g min^{-1}	K_i^h μM	K_{is}^i μM	mechanism
14	<i>B. subtilis</i> LS	16 \pm 2	1.6 \pm 0.1	26 \pm 3		competitive
	<i>S. pombe</i> LS	2.3 \pm 0.2	5.1 \pm 0.1	2.0 \pm 0.2		competitive
	<i>M. tuberculosis</i> LS	36 \pm 3	0.2 \pm 0.01	11 \pm 2	62 \pm 23	mixed
	<i>E. coli</i> RS	2.8 \pm 0.2	4.8 \pm 0.1	2.7 \pm 0.4	32 \pm 8	partial
	<i>M. tuberculosis</i> RS	2.8 \pm 0.2	0.18 \pm 0.003	0.56 \pm 0.14	4.7 \pm 1.8	partial
15	<i>B. subtilis</i> LS	16 \pm 2	1.08 \pm 0.06	2.6 \pm 0.2		competitive
	<i>S. pombe</i> LS	0.59 \pm 0.06	1.66 \pm 0.02	0.16 \pm 0.01		competitive
	<i>M. tuberculosis</i> LS	30 \pm 4	0.19 \pm 0.01	31 \pm 11	57 \pm 24	partial
	<i>E. coli</i> RS	5.7 \pm 0.5	4.0 \pm 0.2	47 \pm 14	122 \pm 52	partial
	<i>M. tuberculosis</i> RS	4.9 \pm 0.3	0.25 \pm 0.01	2.5 \pm 0.1		competitive
11	<i>B. subtilis</i> LS	12 \pm 2	1.2 \pm 0.1	16 \pm 1		competitive
	<i>M. tuberculosis</i> LS	52 \pm 6	0.18 \pm 0.01	13 \pm 1		competitive
	<i>E. coli</i> RS	2.6 \pm 0.3	8.7 \pm 0.2	8.0 \pm 1.9	65 \pm 19	mixed
	<i>M. tuberculosis</i> RS	18 \pm 2	0.40 \pm 0.02	4.2 \pm 0.3		competitive
12	<i>B. subtilis</i> LS	14 \pm 1	1.03 \pm 0.03	309 \pm 52		competitive
	<i>M. tuberculosis</i> LS	52 \pm 2	0.19 \pm 0.01	220 \pm 16		competitive
	<i>E. coli</i> RS	2.0 \pm 0.2	5.5 \pm 0.1	37 \pm 5	860 \pm 270	partial
	<i>M. tuberculosis</i> RS	20 \pm 2	0.36 \pm 0.02	8.4 \pm 0.6		competitive
13	<i>B. subtilis</i> LS	14 \pm 1	1.03 \pm 0.05		> 1000	uncompetitive
	<i>M. tuberculosis</i> LS	58 \pm 5	0.19 \pm 0.01	357 \pm 63		competitive
	<i>E. coli</i> RS	2.4 \pm 0.2	8.4 \pm 0.1		> 1000	uncompetitive
	<i>M. tuberculosis</i> RS	22 \pm 3	0.38 \pm 0.02		> 1000	uncompetitive

^a Recombinant β_{60} capsid from *B. subtilis*. ^b Recombinant homopentameric lumazine synthase from *S. pombe*. ^c Recombinant homopentameric lumazine synthase from *M. tuberculosis*. ^d Recombinant lumazine synthase from *E. coli*. ^e Recombinant riboflavin synthase from *M. tuberculosis*. The assays with lumazine synthase were performed with substrate **2** held constant, while the concentration of the pyrimidinedione substrate **1** was varied. ^f K_s is the substrate dissociation constant for the equilibrium $\text{E} + \text{S} \rightleftharpoons \text{ES}$. ^g k_{cat} is the rate constant for the process $\text{ES} \rightarrow \text{E} + \text{P}$. ^h K_i is the inhibitor dissociation constant for the process $\text{E} + \text{I} \rightleftharpoons \text{EI}$. ⁱ K_{is} is the inhibitor dissociation constant for the process $\text{ES} + \text{I} \rightleftharpoons \text{ESI}$. The reaction mixture contained 50 mM Tris-HCl, pH 7.0.

**FIGURE 3.** Hypothetical structure of the substrate analogue **14** bound in the active site of *B. subtilis* lumazine synthase. The figure is programmed for walleyed (relaxed) viewing.

The greater inhibitory potency of the *S*-nucleoside **15** and its nitro precursor **14** compared with the *C*-nucleoside **13** and its nitro precursor **12** could possibly be due to electronics. The nonbonded electrons on the sulfur may delocalize into the ring, and this may increase its activity relative to the carbon analogue **13**. The electronic factor would cause **15** to more closely resemble the natural substrate relative to the *C*-nucleoside analogue **13**. This might also explain why the nitro *S*-nucleoside compound **14** is more active than the nitro *C*-nucleoside compound **12**.

The significance of the results can be summarized in the following points: (1) The methods used to prepare **14** and **15** could most likely be generalized to allow the synthesis of additional *S*-nucleoside derivatives. (2) Since the *S*-nucleoside analogue **15** of the corresponding natural *N*-nucleoside substrate **1** is active as a lumazine synthase inhibitor, one can conclude

that the inactivity of the *C*-nucleoside analogue **13** is probably related to its lack of a nonbonded electron pair on the carbon atom in question. (3) The substrate analogue **15** inhibits lumazine synthases from a number of important human pathogens, including *M. tuberculosis* and *C. albicans*. The target compound and its synthetic nitro precursor are also inhibitors of *E. coli* riboflavin synthase. The present expansion of the series of known lumazine synthase and riboflavin synthase inhibitors will aid in the future drug design efforts.^{16,23–35} (4) An antibiotic that could inhibit two essential enzymes would theoretically

(23) Al-Hassan, S. S.; Kulick, R. J.; Livingston, D. B.; Suckling, C. J.; Wood, H. C. S.; Wrigglesworth, R.; Ferone, R. *J. Chem. Soc., Perkin Trans. 1* **1980**, 2645–2656.

(24) Ginger, C. D.; Wrigglesworth, R.; Inglis, W. D.; Kulick, R. J.; Suckling, C. J.; Wood, H. S. C. *J. Chem. Soc., Perkin Trans. 1* **1984**, 953–958.

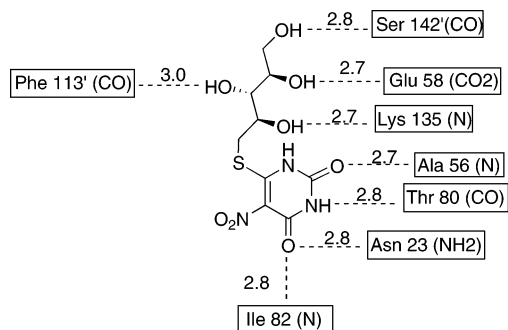


FIGURE 4. Hydrogen bonds and distances (Å) of the substrate analogue **14** bound in the active site of *B. subtilis* lumazine synthase.

delay the emergence of resistant strains, because to become resistant, the microorganism would have to simultaneously mutate two enzymes instead of only one. (5) Finally, the *S*-nucleoside analogue **15** may eventually prove to be valuable in trapping lumazine synthase-bound intermediate analogues of the hypothetical intermediates **6** or **7** for structural and mechanistic studies.

Experimental Section

NMR spectra were determined at 300 MHz (^1H) and 75 MHz (^{13}C) in CDCl_3 or $\text{MeOH-}d_4$. Flash chromatography was performed using 230–400 mesh silica gel. TLC was carried out using commercially available precoated glass silica gel plates of 250 μm thickness. TLC plates were developed using anisaldehyde staining solution. Melting points are uncorrected. Unless otherwise stated, chemicals and solvents were of reagent grade and obtained from commercial sources without further purification. Solvents were dried and distilled following usual protocols.

5-Nitro-6-D-ribylthiopyrimidine-2,4(1H,3H)-dione (14). **Method A.** TMSI (50 μL , 0.36 mmol) was added to a solution of ribitylthiopyrimidine derivative **23** (30 mg, 0.072 mmol) in dry acetonitrile (2 mL), and the reaction mixture was stirred for 16 h at rt. The orange-red solution was diluted with H_2O (5 mL) and washed with CH_2Cl_2 (3 \times 5 mL). The colorless aqueous layer was evaporated, and the residue was purified by flash silica gel column chromatography, eluting with 8% methanol in ethyl acetate to yield compound **14**, which was further washed with THF (3 \times 10 mL)

to give yellowish solid compound **14** (12 mg, 55%). **Method B.** HCl (1 N, 2 mL) was added to a solution of compound **25** (30 mg, 0.074 mmol) in MeOH (2 mL), and the reaction mixture was stirred for 12 h at rt. MeOH was removed under vacuum to yield yellowish solid **14** (17 mg, 71%): mp 225–228 $^\circ\text{C}$ dec; $[\alpha]_D^{25} +39$ (c 0.4, MeOH); $^1\text{H NMR}$ (300 MHz, $\text{MeOH-}d_4$) δ 4.58 (m, 1 H), 4.01 (m, 1 H), 3.79 (m, 1 H), 3.65 (m, 2 H), 3.43 (dd, $J = 2.4, 14.0$ Hz, 1 H), 3.15 (dd, $J = 7.8, 14.3$ Hz, 1 H); $^{13}\text{C NMR}$ (75 MHz, $\text{MeOH-}d_4$) δ 176.9, 161.5, 157.4, 122.9, 75.4, 74.1, 73.6, 64.6, 35.5; ESI-MS (negative mode) m/z (rel intensity) 322 $[(\text{M} - \text{H})^-]$, 100], 172 (10). Anal. Calcd for $\text{C}_9\text{H}_{13}\text{N}_3\text{O}_8\text{S}$: C, 33.44; H, 4.05; N, 13.00; S, 9.92. Found: C, 33.69; H, 3.98; N, 12.97; S, 9.78.

5-Amino-6-(D-ribylthio)pyrimidine-2,4(1H,3H)-dione Hydrochloride (15). HCl (1 N, 1 mL) was added to a solution of compound **26** (25 mg, 0.067 mmol) in MeOH (1 mL), and the reaction mixture was stirred for 12 h at rt. MeOH was removed under vacuum, and the residue was crystallized from MeOH and diethyl ether to afford compound **15** (14 mg, 64%): mp 137–139 $^\circ\text{C}$ dec; $[\alpha]_D^{25} +14$ (c 0.4, MeOH); $^1\text{H NMR}$ (300 MHz, $\text{MeOH-}d_4$) δ 4.07 (m, 1 H), 3.82–3.60 (m, 4 H), 3.47–3.33 (m, 2 H); $^{13}\text{C NMR}$ (75 MHz, $\text{MeOH-}d_4$) δ 160.4, 151.2, 150.1, 106.5, 74.4, 74.1, 72.9, 64.4, 37.8; EIMS m/z (rel intensity) 587 (2MH^+ , 72), 294 (MH^+ , 100); ESI-MS (negative mode) m/z (rel intensity) 585 $[(2\text{M} - \text{H})^-]$, 91], 292 $[(\text{M} - \text{H})^-]$, 100], 158 (37). Anal. Calcd for $\text{C}_9\text{H}_{16}\text{ClN}_3\text{O}_6\text{S}$: C, 32.78; H, 4.89; N, 12.74; S, 9.72. Found: C, 33.09; H, 5.11; N, 12.58; S, 10.05.

Thioacetyl-2,3,4,5-di-O-isopropylidene-D-ribose (19). Triethylamine (0.24 mL, 1.72 mmol), 4-(dimethylamino)pyridine (126 mg, 1.03 mmol), and *p*-toluenesulfonyl chloride (180 mg, 0.95 mmol) were added to a solution of D-ribose derivative **17** (0.2 g, 0.86 mmol) in dry pyridine (4 mL), and the mixture was stirred under argon at 0 $^\circ\text{C}$ for 24 h. The orange-red reaction mixture was extracted with diethyl ether (25 mL), and the extract was washed with water. The ether solution was dried and evaporated under high vacuum, and the tosyl derivative **18** was used without purification for the next step. Crude **18** (0.33 g, 0.85 mmol) was dissolved in dry acetonitrile (5 mL) under argon. The solution was cooled to 0 $^\circ\text{C}$, potassium thioacetate (0.29 g, 2.56 mmol) was added, and the reaction mixture was heated at reflux for 3 h. The reaction mixture was diluted with CHCl_3 (25 mL), washed with water and brine, dried, and evaporated, and the residue was purified by flash silica gel chromatography, eluting with 15% ethyl acetate in hexane, to give the thioacetylated compound **19** (0.19 g, 76% from **17**) as a colorless oil: $^1\text{H NMR}$ (300 MHz, CDCl_3) δ 4.24 (m, 1 H), 4.11 (m, 2 H), 3.96 (m, 1 H), 3.90 (m, 1 H), 3.52 (dd, $J = 4.2$ Hz, 1 H), 3.04 (dd, $J = 9.6$ Hz, 1 H), 2.33 (s, 3 H), 1.40 (s, 3 H), 1.39 (s, 3 H), 1.32 (s, 3 H), 1.30 (s, 3 H). Anal. Calcd for $\text{C}_{13}\text{H}_{22}\text{O}_5\text{S}$: C, 53.77; H, 7.64; S, 11.04. Found: C, 53.98; H, 7.61; S, 10.81.

2,3,4,5-Di-O-isopropylidene-D-ribylthiol (20). Thioacetyl derivative **19** (100 mg, 0.33 mmol) was dissolved in dry methanol (3 mL) and cooled to 0 $^\circ\text{C}$, and then sodium methoxide (5 mg) was added. The reaction mixture was stirred for 12 h under argon, acidified with acetic acid, and filtered through Celite. The filtrate was concentrated to dryness. The residue was purified by flash silica gel column chromatography, eluting with 10% ethyl acetate in hexane to yield compound **20** (60 mg, 70%) as a colorless oil: $^1\text{H NMR}$ (300 MHz, CDCl_3) δ 4.27 (ddd, $J = 5.1, 8.4, 8.4$ Hz, 1 H), 4.05 (m, 3 H), 3.89 (m, 1 H), 2.79 (m, 2 H), 1.84 (dd, $J = 7.2, 9.6$ Hz, 1 H), 1.41 (s, 6 H), 1.34 (s, 3 H), 1.33 (s, 3 H); EIMS m/z (rel intensity) 248 (M^+ , 1.1), 101 ($\text{M}^+ - \text{C}_6\text{H}_{11}\text{O}_2\text{S}$, 74), 59 ($\text{MH}^+ - \text{C}_8\text{H}_{14}\text{O}_3\text{S}$, 100); CIMS m/z (rel intensity) 249 (MH^+ , 99), 233 ($\text{M}^+ - \text{H}_2\text{O}$, 23), 191 (M^+ , 100). Anal. Calcd for $\text{C}_{11}\text{H}_{20}\text{O}_4\text{S}$: C, 53.20; H, 8.12; S, 12.91. Found: C, 53.01; H, 8.09; S, 12.77.

Further elution gave compound **21** (15 mg, 9%) as a colorless oil: $^1\text{H NMR}$ (300 MHz, CDCl_3) δ (dt, $J = 4.2, 9.1$ Hz, 1 H), 4.04 (m, 1 H), 3.96 (m, 2 H), 3.84 (m, 1 H), 3.45 (dd, $J = 3.6, 13.3$ Hz, 1 H), 2.85 (dd, $J = 9.1, 13.3$ Hz) 1.36 (s, 3 H), 1.33 (s, 3 H), 1.29 (s, 3 H), 1.26 (s, 3 H); EIMS m/z (rel intensity) 494 (M^+ , 3.4), 247

(25) Wrigglesworth, R.; Inglis, W. D.; Livingstone, D. B.; Suckling, C. J.; Wood, H. C. S. *J. Chem. Soc., Perkin Trans. 1* **1984**, 959–963.

(26) Cushman, M.; Patrick, D. A.; Bacher, A.; Scheuring, J. *J. Org. Chem.* **1991**, *56*, 4603–4608.

(27) Cushman, M.; Mavandadi, F.; Kugelbrey, K.; Bacher, A. *J. Org. Chem.* **1997**, *62*, 8944–8947.

(28) Cushman, M.; Mihalic, J. T.; Kis, K.; Bacher, A. *J. Org. Chem.* **1999**, *64*, 3838–3845.

(29) Cushman, M.; Mavandadi, F.; Yang, D.; Kugelbrey, K.; Kis, K.; Bacher, A. *J. Org. Chem.* **1999**, *64*, 4635–4642.

(30) Cushman, M.; Yang, D.; Kis, K.; Bacher, A. *J. Org. Chem.* **2001**, *66*, 8320–8327.

(31) Cushman, M.; Yang, D.; Gerhardt, S.; Huber, R.; Fischer, M.; Kis, K.; Bacher, A. *J. Org. Chem.* **2002**, *67*, 5807–5816.

(32) Cushman, M.; Yang, D.; Mihalic, J. T.; Chen, J.; Gerhardt, S.; Huber, R.; Fischer, M.; Kis, K.; Bacher, A. *J. Org. Chem.* **2002**, *67*, 6871–6877.

(33) Cushman, M.; Sambaiah, T.; Jin, G.; Illarionov, B.; Fischer, M.; Bacher, A. *J. Org. Chem.* **2004**, *69*, 601–612.

(34) Cushman, M.; Jin, G.; Illarionov, B.; Fischer, M.; Ladenstein, R.; Bacher, A. *J. Org. Chem.* **2005**, *70*, 8162–8170.

(35) Zhang, Y.; Illarionov, B.; Bacher, A.; Georg, G. I.; Ye, Q.-Z.; Vander Velde, D.; Fanwick, P. E.; Song, Y.; Cushman, M. *J. Org. Chem.* **2007**, *72*, 2769–2776.

($M^+ - C_{11}H_{19}O_4S$, 3), 101 ($M^+ - C_{17}H_{29}O_6S_2$, 98), 59 ($M^+ - C_{19}H_{32}O_7S_2$, 100); CIMS m/z (rel intensity) 494 (M^+ , 16), 379 ($MH^+ - C_6H_{10}O_2$, 100); HRMS m/z calcd for $C_{22}H_{38}O_8S_2$ 494.2008, found 494.2006.

4-(2,3:4,5-Di-*O*-isopropylidene-*D*-ribitylthio)-2,6-dimethoxy-5-nitropyrimidine (23). A solution of *D*-ribitylthio derivative **20** (40 mg, 0.16 mmol) and iodopyrimidine derivative **22**^{19,20} (50 mg, 0.16 mmol) in dry DMF (2 mL) was cooled to 0 °C, and K_2CO_3 (66 mg, 0.48 mmol) was added. The solution was stirred overnight at rt. The reaction mixture was diluted with H_2O (15 mL) and extracted with diethyl ether (2 × 10 mL). The ether layer was washed with brine, dried, and concentrated. The residue was purified by flash silica gel column chromatography, eluting with 5% ethyl acetate in hexane, to yield an amorphous solid compound **23** (60 mg, 86%): mp 102–104 °C; 1H NMR (300 MHz, $CDCl_3$) δ 4.46 (dt, $J = 4.5, 9.1$ Hz, 1 H), 4.14 (m, 2 H), 4.09 (s, 3 H), 4.07 (s, 3 H), 4.01 (m, 2 H), 3.79 (dd, $J = 4.5, 13.8$ Hz, 1 H), 3.15 (dd, $J = 9.0, 13.8$ Hz, 1 H), 1.55 (s, 3 H), 1.42 (s, 3 H), 1.40 (s, 3 H), 1.33 (s, 3 H); ^{13}C NMR (75 MHz, $CDCl_3$) δ 170.9, 165.1, 161.9, 126.0, 109.9, 109.2, 78.7, 75.8, 73.2, 68.0, 56.0, 55.7, 31.6, 28.0, 26.7, 25.4; EIMS m/z (rel intensity) 432 (M^+ , 100), 214 ($M^+ - C_6H_7N_3O_4S$, 46), 101 ($C_5H_9O_2^+$, 26); CIMS m/z (rel intensity) 416 ($M^+ - CH_3$, 17), 101 ($C_5H_9O_2^+$, 100). Anal. Calcd for $C_{17}H_{25}N_3O_8S$: C, 47.32; H, 5.84; N, 9.74; S, 7.43. Found: C, 47.02; H, 5.69; N, 9.97; S, 7.61.

6-(2,3:4,5-Di-*O*-isopropylidene-*D*-ribitylthio)-5-nitropyrimidine-2,4(1*H*,3*H*)-dione (25). Thioacetate compound **19** (24 mg, 0.08 mmol) was dissolved in MeOH (3 mL), and MeONa (18 mg, 0.32 mmol) was added to the reaction mixture. The reaction mixture was stirred at rt for 1 h, 6-chloro-5-nitrouacil (16 mg, 0.08 mmol) was introduced, and the mixture was heated at reflux overnight under argon atmosphere. The reaction mixture was cooled and concentrated, and the residue was purified by flash silica gel chromatography, eluting with 80% ethyl acetate in hexane, to yield an oily compound **25** (20 mg, 59%): 1H NMR (300 MHz, MeOH- d_4) δ 4.62 (brs, 1 H), 4.46 (m, 1 H), 4.22 (m, 1 H), 4.08 (m, 2 H), 3.91 (dd, $J = 5.7$ Hz, 8.9 Hz, 1 H), 3.52 (dd, $J = 4.5$ Hz, 13.6 Hz, 1 H), 3.24 (dd, $J = 9.0$ Hz, 13.6 Hz, 1 H), 1.40 (s, 3 H), 1.38 (s, 3 H), 1.31 (s, 3 H), 1.29 (s, 3 H); ^{13}C NMR (75 MHz, MeOH- d_4) δ 161.3, 157.4, 122.3, 111.1, 109.8, 80.0, 77.5, 74.7, 68.5, 32.0, 30.8, 28.3, 27.1, 25.7; EIMS m/z (rel intensity) 829 ($2MNa^+$, 25), 448 (MNa^+ , 100), 426 (79); ESI-MS (negative mode) m/z (rel intensity) 827 [$(2M - 2H)^-$, 100], 403 (M, 14), 402 [$(M - H^+)^-$, 83]. Anal. Calcd for $C_{15}H_{21}N_3O_8S \cdot 2.75H_2O$: C, 39.78; H, 5.90; N, 9.28. Found: C, 39.94; H, 5.85; N, 8.98.

5-Amino-6-(2,3:4,5-di-*O*-isopropylidene-*D*-ribitylthio)pyrimidine-2,4(1*H*,3*H*)-dione (26). Sodium bicarbonate/sodium carbonate buffer (2 mL, pH = 9, prepared by adjusting the pH of a saturated aqueous sodium bicarbonate solution to 9 with sodium carbonate and 1 M NaOH) and $Na_2S_2O_4$ (130 mg, 1.5 mmol) were added to a solution of compound **25** (60 mg, 0.15 mmol) in 1,4-dioxane (3 mL). Argon was bubbled for 30 min to degas the reaction mixture, which was then stirred at rt for 6 h and subsequently at 100 °C for 2 h. The reaction mixture was cooled to rt, poured into ice-water (5 mL), and extracted with diethyl ether (3 × 8 mL). The organic layer was combined, washed with brine, and dried, and solvent was distilled off. The residue was purified by flash silica gel column chromatography, eluting with 20% ethyl acetate in hexane to yield compound **26** (45 mg, 82%) as a pale yellow solid: mp 148–150 °C dec; 1H NMR (300 MHz, MeOH- d_4) δ 4.39 (m, 1 H), 4.13 (m, 2 H), 4.04 (m, 1 H), 3.87 (m, 1 H), 3.25 (dd, $J = 3.6$ Hz, 14.0 Hz, 1 H), 3.10 (dd, $J = 9.5$ Hz, 14.0 Hz, 1 H), 1.38 (s, 3 H), 1.37 (s, 3 H), 1.32 (s, 3 H), 1.31 (s, 3 H); ^{13}C NMR (75 MHz, MeOH- d_4) δ 161.8, 151.4, 127.4, 122.3, 111.2, 110.3, 79.9, 78.7, 74.5, 68.8, 34.8, 28.1, 27.0, 25.6; ESI-MS (negative mode) m/z (rel intensity) 373 (M, 81), 372 [$(M - H^+)^-$, 100], 315 (30), 314 (38). Anal. Calcd for $C_{15}H_{23}N_3O_6S$: C, 48.25; H, 6.21; N, 11.25; S, 8.59. Found: C, 48.34; H, 6.18; N, 11.43; S, 8.71.

TABLE 2. Enzymes Used in Kinetic Assays

enzyme	organism	specific activity ($\mu M \text{ mg}^{-1} \text{ h}^{-1}$)	concn of enzyme in reaction mixture ($\mu g \text{ mL}^{-1}$)
lumazine synthases:			
	<i>B. subtilis</i>	7.5	2.0
	<i>S. pombe</i>	7.6	1.0
	<i>M. tuberculosis</i>	0.9	30
riboflavin synthases:			
	<i>E. coli</i>	19	0.8
	<i>M. tuberculosis</i>	3.0	4.0

Molecular Modeling. Using Sybyl (Tripos, Inc., version 7.0), the X-ray crystal structure of the complex of 5-nitro-6-ribitylamino-2,4(1*H*,3*H*)-pyrimidinedione (**11**)¹⁵ with *B. subtilis* lumazine synthase was clipped to include information within a 12 Å radius sphere of one of the 60 equiv ligand molecules. The residues that were clipped in this cut complex were capped with either neutral amino or carboxyl groups. Inhibitor **14** was overlapped with the structure of 5-nitro-6-ribitylamino-2,4(1*H*,3*H*)-pyrimidinedione (**11**), which was then deleted. Hydrogen atoms were added to the complex. MMFF94 charges were loaded, and the energy of the complex was minimized using the Powell method to a termination gradient of 0.05 kcal/mol employing the MMFF94s force field. During the minimization of the complex, inhibitor **14** and a 6 Å radius sphere surrounding it were allowed to remain flexible, while the remaining portion of the complex was held rigid using the aggregate function. Figure 3 was constructed by displaying the amino acid residues of the enzyme involved in hydrogen bonding with the inhibitor **14**. The maximum distance between the heavy atoms participating in the hydrogen bonds shown in Figure 3 was set at 3.6 Å.

Kinetic Assays. All assays were performed in 96-well microtiter plates using a computer-controlled SpectraMax 2 microplate reader (Molecular Devices GmbH, Ismaning, Germany). Enzymes used in kinetic assays are specified in Table 2.

Lumazine Synthase Assay. Assay mixtures contained 50 mM Tris hydrochloride, pH 7.0, 100 mM NaCl, 2% (v/v) DMSO, 5 mM dithiothreitol, 100 μM **2**, lumazine synthase, and **1** (3–150 μM) in a volume of 0.2 mL. Assay mixtures were prepared as follows. A solution (175 μL) containing 103 mM NaCl, 5.1 mM dithiothreitol, 114 μM **2**, and lumazine synthase in 51 mM Tris hydrochloride, pH 7.0, was added to 4 μL of inhibitor in 100% (v/v) DMSO (inhibitor concentration window, 0–300 μM) in a well of a 96-well microtiter plate. The reaction was started by adding 21 μL of a solution containing 103 mM NaCl, 5.1 mM dithiothreitol, and substrate **1** (30–1500 μM) in 51 mM Tris hydrochloride, pH 7.0. The formation of 6,7-dimethyl-8-*D*-ribityllumazine (**3**) was monitored photometrically (408 nm; $\epsilon_{\text{lumazine}} = 10,200 \text{ M}^{-1} \text{ cm}^{-1}$) for a period of 40 min at 27 °C.

Riboflavin Synthase Assay. Assay mixtures contained 50 mM Tris hydrochloride, pH 7.0, 100 mM NaCl, 2% (v/v) DMSO, 5 mM dithiothreitol, enzyme, and variable concentrations of **3** (3–20 μM) in a volume of 0.2 mL. Assay mixtures were prepared as follows. A solution (175 μL) containing 103 mM NaCl, 5.1 mM dithiothreitol, and riboflavin synthase in 51 mM Tris hydrochloride, pH 7.0, was added to 4 μL of inhibitor in 100% (v/v) DMSO (inhibitor concentration window, 0–400 μM) in a well of a 96-well microtiter plate. The reaction was started by adding 21 μL of a solution containing 103 mM NaCl, 5.1 mM dithiothreitol, and substrate **3** (30–200 μM) in 51 mM Tris hydrochloride, pH 7.0. The formation of riboflavin was monitored photometrically (470 nm; $\epsilon_{\text{riboflavin}} = 9600 \text{ M}^{-1} \text{ cm}^{-1}$) for a period of 40 min at 27 °C.

Evaluation of Kinetic Data. The velocity–substrate data were fitted for all inhibitor concentrations with a nonlinear regression method using the program DynaFit.³⁶ Different inhibition models were considered for the calculation. K_i and K_{is} values \pm standard

(36) Kuzmic, P. *Anal. Biochem.* **1996**, *237*, 260–273.

deviations were obtained from the fit under consideration of the most likely inhibition model as described previously.³⁴

Acknowledgment. This research was made possible by NIH grants GM51469 and R21 NS053634 as well as by support from the Fonds der Chemischen Industrie and the Hans Fischer Gesellschaft. This research was conducted in a facility constructed with support from Research Facilities Improvement

Program Grant No. C06-14499 from the National Center for Research Resources of the National Institutes of Health.

Supporting Information Available: ¹H NMR and ¹³C NMR spectra. This material is available free of charge via the Internet at <http://pubs.acs.org>.

JO0709495